JOURNAL OF Applied Polymer SCIENCE

Effect of Take-Up Speed on Polyvinylidene Fluoride Hollow Fiber Membrane in a Thermally Induced Phase Separation Process

Xianfeng Li,[1] Huiyu Liu,[2] Changfa Xiao,[1] Shihu Ma,[1] Xuehui Zhao[1]

[1]State Key Laboratory of Hollow Fiber Membrane Materials and Processes, School of Materials Science and Engineering, Tianjin Polytechnic University, Tianjin 300160, People's Republic of China

[2]Technical Institute of Physics and Chemistry of CAS, Beijing 100190, People's Republic of China

Correspondence to: C. Xiao (E-mail: cfxiao@tjpu.edu.cn)

ABSTRACT: The porous polyvinylidene fluoride hollow fiber membranes were prepared via the thermally induced phase separation process using mixed diluent. The effects of take-up speed on the structure of membranes were investigated by scanning electron microscopy, differential scanning calorimetry, and wide-angle X-ray diffraction. The membrane properties were measured in terms of the pure water flux, porosity, and mechanical properties. The results showed that the cross-sectional structure of membrane had an obvious change and presented a uniform structure when TS increased to 72 m min^{-1}, whereas the membrane made from TS <41 m min^{-} presented an interconnected aggregation structure. However, the change of surface structure of all membranes was hardly observed. In addition, the strength and elongation of breakage of membrane increased obviously with the increase of TS, whereas the pure water flux and porosity changed slightly. © 2012 Wiley Periodicals, Inc. J. Appl. Polym. Sci. 000: 000–000, 2012

KEYWORDS: polyvinylidene fluoride (PVDF); hollow fiber membrane; thermally induced phase separation (TIPS); take-up speed (TS); structure

Received 17 March 2011; accepted 19 April 2012; published online
DOI: 10.1002/app.37919

INTRODUCTION

The thermally induced phase separation (TIPS) process is a valuable way of making microporous membrane. Polyvinylidene fluoride (PVDF) presents an outstanding physical and chemical property. Therefore, researchers pay more and more attention to preparing PVDF porous membrane by TIPS method.[1–17] However, it is very difficult to prepare PVDF membrane with good properties using TIPS method because few kinds of single solvent in industrial products can be selected as the diluents. The authors[16,17] prepared PVDF flat sheet membrane with uniform porous structure via adopting mixed diluents (MDs). However, the hollow fiber membrane is one of the most useful membrane forms from the commercial application because it enables higher membrane area per unit membrane module volume. However, less investigation lies on PVDF hollow fiber membrane which needs a more complex technical. Recently, to improve performance membrane, Cha and Yang[18] prepared PVDF hollow fiber membranes using modified TIPS process based on PVDF/γ-butyrolactone system, and the particulate structure was formed. Ji et al.[19] investigated the effects of the MDs on the structure and property of the PVDF hollow fiber membranes using dibutyl phthalate (DBP)/di(2-ethylhexyl) phthalate as MD and liquid paraffin as the bore liquid. The membrane formation mechanism of hollow fiber membranes was proposed. Matsuyama and coworkers[20,21] prepared PVDF hollow fiber membrane with different structures, which was applied for gas–liquid membrane contactors.

In the fabrication of hollow fiber membranes, a high-speed spinning is important to maximize the productivity and minimize the production cost. In chemical fiber industry, high take-up speed (TS) is used to improve the mechanical property of fiber owing to good orientation and crystallization.[22] For the diffusion-induced phase separation process (DIPS), Chung[23] found that the increase in the TS resulted in the deformation of inner shapes of the fibers. Matsuyama et al.[24] found that the effect of TS on the permeability of poly(ethylene-*co*-vinyl alcohol) (EVAL) membrane is more sensitive at the high-temperature cooling bath. However, for the effect of TS on the hollow fiber membrane in TIPS process, little investigation is performed systematically.

In this article, porous PVDF hollow fibers were prepared using DBP and dioctyl phthalate (DOP) as MD by TIPS method. The effects of TS on the structure and property of membrane were

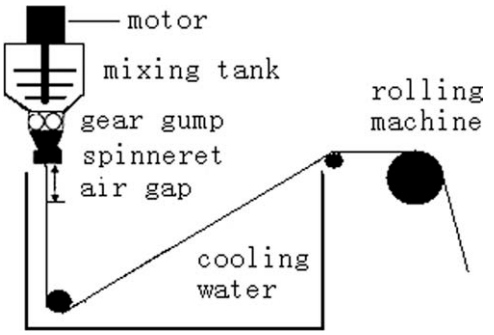

Figure 1. Schematic diagram of hollow fiber membrane extrusion machine.

investigated in detail. It would provide some information to improve the membrane property and industrialize membrane product.

EXPERIMENTAL

Materials

PVDF (solef1010, melt flow index 2 at 2.16 kg) was supplied by Solvay (France). Both DBP (density 1.046 g cm^{-3}; boiling point 340°C) and DOP (density 0.985 g cm^{-3}; boiling point 370°C) are analytical reagent, bought from Tianjin Yongda Chemical Reagent (China). Ethanol was obtained from common industrial product suppliers.

Preparation of Hollow Fiber Membranes

MD (V_{DBP}/V_{DOP}, 1/1) and PVDF (PVDF concentration 28.6wt %) were weighed into a mixing tank, which was tumbled on a roller machine for 4 h maintained in a 220°C environment until a homogeneous solution was formed. The solution was spun via gear pump after degas, cooled first via a 10-cm-long room temperature air gap, then cooled in a same temperature water bath, formed hollow fiber. Spinning process is shown in Figure 1 in which extruding rate was 24 g min^{-1}. The bore fluid was 130°C DOP.

Characterization of Hollow Fiber Membrane

Structure. MD remained on the newly formed membrane was extracted by ethanol and membranes were dried in air, and fractured in liquid nitrogen. The surface and cross-sectional morphologies of membrane were coated with gold, observed using a scanning electron microscopy (SEM, Quanta 200, Netherlands FEI).

Pure Water Flux. After the diluent was extracted by ethanol, the hollow fiber was post-treated by dipping in a 50 wt % aqueous glycerol solution for 48 h and dried in air at room temperature to make the test modules. Then pure water flux (PWF) was tested through inner pressure method on a test module which consisted of 20 fibers with 15 cm length each. The transmembrane pressure was 0.1 MPa. Three modules were tested and their average result was reported. PWF was determined by the following equation

$$J = Q/(AT) \tag{1}$$

where J is PWF ($L{\cdot}m^{-2}{\cdot}h^{-1}$), Q the quantity of the permeate (L), T the sampling time (h), and A is the membrane area (m^2).

Porosity. The membrane porosity (ε) is defined as the pore volume divided by the total volume of the porous membrane. It can be determined by gravimetric method:

$$\varepsilon = \frac{(W_w - W_d)/\rho_w}{(W_w - W_d)/\rho_w + W_d/\rho_P} \times 100\% \tag{2}$$

where W_w and W_d are the weights of the wet and dry membranes, respectively. ρ_w is the water density and ρ_P, the polymer density (1.78 g cm^{-3}).

Differential Scanning Calorimetry. A differential scanning calorimetry (DSC) (Perkin-Elmer, DSC-7) was used to determine the characteristics of crystallization. About 10 mg sample was sealed in an aluminum DSC pan, and the DSC was also obtained at 10°C min^{-1} heat rate. Melt heat ΔH_m was determined from the melting peak area. Crystallinity was evaluated by

$$\Phi_{DSC} = \Delta H_m/\Delta H_{100} \tag{3}$$

ΔH_{100} = 104.7J g^{-1} is the melting heat for a 100% crystalline sample of PVDF.[25]

Wide-Angle X-ray Diffraction. The wide-angle X-ray diffraction (WAXD) of the samples was recorded by Bruker AXS D8 DISCOVER with GADDS (Madison, USA) for investigating polymorphism of PVDF crystals. Cu K-α radiation (λ = 1.5418 Å) was employed.

Mechanical Properties. The 250-mm-long fiber samples were tested at room temperature using an electronic single-yarn strength tester (PC-YG061, Laizhou, China) on the basis of National Standard of China (GB/T 3916-1997), and the tensile rate was 250 mm min^{-1}. The stress was then calculated by pull force (N) and linear density of fiber (tex), For each specimen, no less than four runs were performed and representative sample properties were exhibited. Break strength (MPa) came from the testing stress value (N/tex) supposing a constant PVDF density (ρ_{PVDF} = 1.78 g cm^{-3}).

Shrinkage Rate. The shrinkage rate is an important property when dry membrane is need; for example, the preparation of hydrophobic membrane and module. Hence, the shrinkage rate (S) was measured by:

$$S = (L_w - L_d)/L_w \tag{4}$$

L_w and L_d is the lengths of wet and dry membrane samples, and The five samples (20-cm long each) were measured, and the average values were presented.

RESULTS AND DISCUSSION

Membrane Structure

The effects of TS on the cross-sectional structure of hollow fiber are shown in Figure 2. It can be seen that when TS is lower than 41 m min^{-1}, the cross-sectional structure does not change much. All present an interconnected aggregation structure, and moreover, the aggregations become gradationally smaller in size from the inner surface to outer surface, that is the membranes

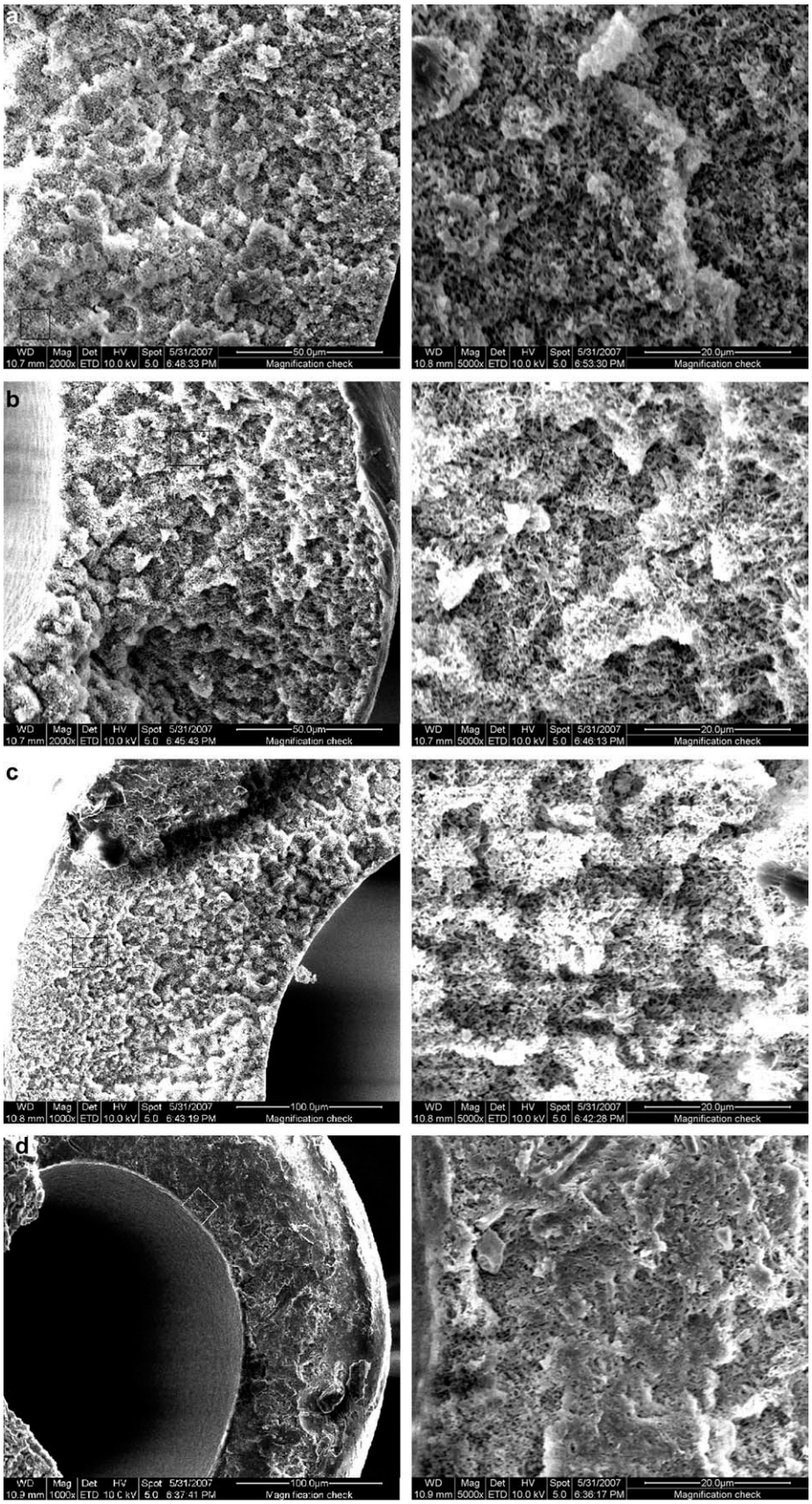

Figure 2. Cross-sectional structure of hollow fibers (a, 20; b, 30; c, 41; d, 72 m min^{-1}).

Applied Polymer SCIENCE

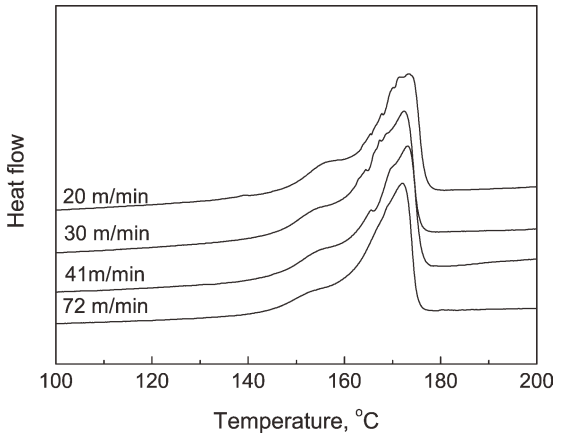

Figure 3. DSC curves of hollow fibers.

present an asymmetric structure. However, when TS reaches 72 m min^{-1}, an obvious change in membrane structure occurs. The asymmetric structure disappears. Instead, the whole cross-section exhibits a more uniform structure. From observation through SEMs, it seems that the porosity of the membrane decreases. Coincidently, there is also an obvious change in the pattern of DSC curves (Figure 3) when TS reaches 72 m min^{-1}. Only the DSC curve of the fourth sample (72 m min^{-1}) is smooth, and distinguished from the other curves.

In spinning process, different cooling conditions were adopted for the outside and inside of hollow fiber. Crystallization studies show[14] that the rate of cooling determines the number and size of crystallites. Slower cooling rates give a polymer chain more opportunity to disentangle during crystallization, increase the size and perfection of the crystals. The high crystallization heat by DSC at slow cooling rate also confirms this result.[14] Hence, the aggregation size becomes gradationally smaller from the inner surface to outer surface. This leads to an asymmetric structure. This result also appeared in the process of preparing PVDF flat sheet membrane.[16,17]

There would be two reasons that cause obvious change of structure when TS increased to 72 m min^{-1}. First, for TIPS, the membrane structure is influenced obviously by the cooling rate.[14,16,17] When TS increases, the thickness of hollow fiber wall decreases and the cooling rate increases because the

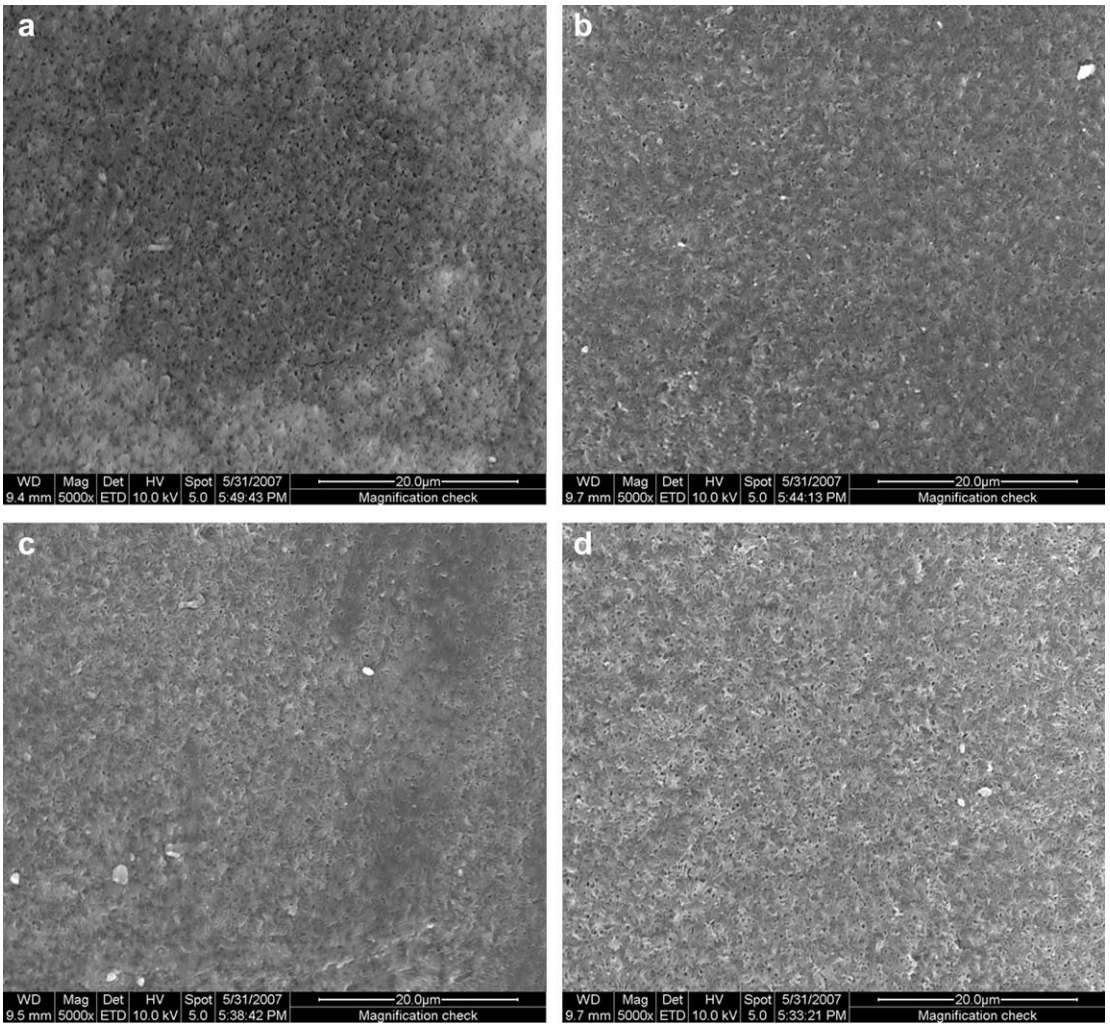

Figure 4. Surface structure of hollow fibers (a, 20; b, 30; c, 41; d, 72 m min^{-1}).

Table I. Effects of TS on the Property of Hollow Fibers

TS (m min^{-1})	Outer/inner diameter (mm)	Flux (L m^{-2} h)	Porosity (%)	Shrinkage rate (%)
20	1.10/0.55	273	70.1	7.0
30	0.83/0.46	274	69.1	7.5
41	0.70/0.36	281	70.3	8.2
72	0.53/0.31	264	66.2	11

extruding rate of PVDF solution and the temperature of cooling bath are constant.

The second reason is the change of elongational stress with the changing of TS in spinning process. It is known, in DIPS process, that an increase in TS results in increasing elongational stress, thus influencing the structure, property,[26,27] and dimension[28,29] of the resultant fibers. Similarly, an increase of TS in TIPS process will result in increasing elongational stress which would also influence PVDF macromolecular state before solidification, and then influence the resulted structure although TIPS process is different than DIPS process. In this article, it seems that the combination of the cooling rate and elongational stress resulted in an obvious change of structure when TS increased to 72 m min^{-1}. The influencing reason is more complex, and needs further experiment and analysis.

The effect of TS on the surface structure shown in Figure 4 is not obvious. All the membranes present a uniform porous structure.

Membrane Properties

Effect of TS on the Inner/Outer Diameter. The effect of TS on the inner/outer diameter of hollow fiber is summarized in Table I. It can be seen that both inner and outer diameters of the fiber decrease with the increase of TS. Moreover, the rate of decrease of outer diameter is faster than that of inner of diameter. Thus, the thickness of membrane wall reduce, which is identical to the literature.[26] The inner and outer diameters of hollow fiber were determined by the extruding rate of PVDF solution, TS, and the flow rate of bore fluid. The drawing ratio of hollow fiber increases when TS increases, and hence the thickness of hollow fiber wall decreases because the extruding rate of PVDF solution and the flow rate of bore fluid are constant.

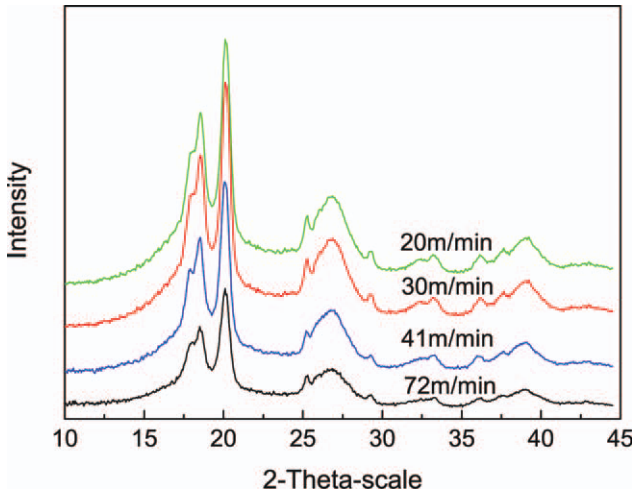

Figure 6. WAXDs of hollow fibers. [Color figure can be viewed in the online issue, which is available at wileyonlinelibrary.com.]

Effect of TS on the PWF and Porosity. Generally, the change of membrane PWF and porosity is minor with the increase of TS (Table I). However, it should be still noted that porosity decreases slightly when TS rises to 72 m min^{-1}, which was also observed under SEM (Figure 2). PWF comes from the membrane pore and thickness. The thickness of membrane decreases when TS rises to 72 m min^{-1}. it is favorable to PWF. However, the porosity decreases which usually influences PWF correspondingly. In addition, the different TS membranes own the similar surface structure. Therefore, PWF changes slightly. Matsuyama[24] also investigated the effect of TS on the permeability of EVAL hollow fiber membranes prepared by TIPS, and found that there are the different effects on different cooling temperature membranes. The effect became weak when the low temperature bath was adopted. In our study, the room temperature cooling bath was used, and then the effect of TS on the water permeability is not obvious.

Effect of TS on the Mechanical Property. The effect of TS on the mechanical property of hollow fiber is shown in Figure 5. With increase of TS, both strength and elongation of breakage increase significantly. The mechanical properties of hollow fiber

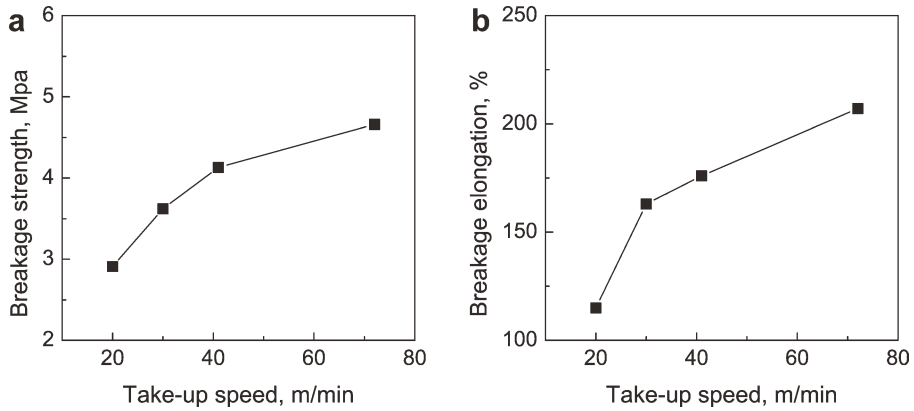

Figure 5. Mechanical property of hollow fibers (a, breakage strength; b, breakage elongation).

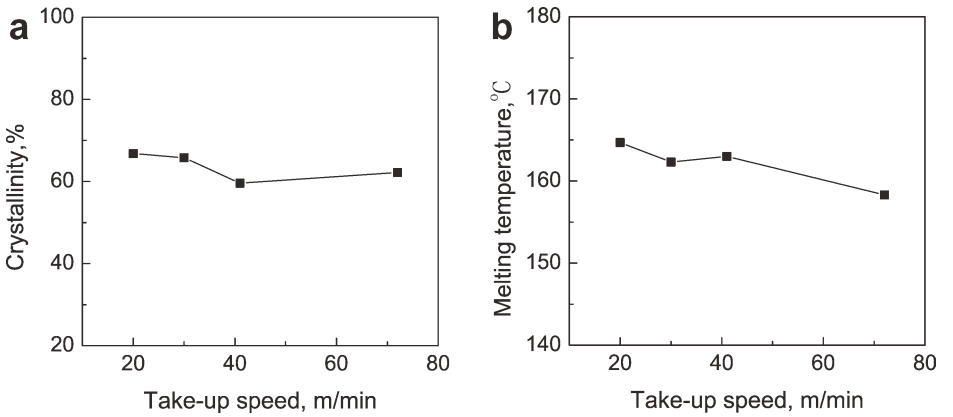

Figure 7. Crystallinity and melting temperature of hollow fibers by DSC.

are closely related to the crystallization of PVDF, which was characterized by DSC (Figure 3) and WAXD (Figure 6). The crystallinity and melting temperature can be calculated from DSC and are shown in Figure 7.[24]

It can be seen clearly that both crystallinity and melting temperature decrease slightly with the increase of TS, that is to say, higher TS results in a lower crystallinity and melting temperature. The same two reasons influence the crystallization of PVDF as influencing structure because the mechanical property is directly related to the structure. One is the cooling rate, and the other is the elongational stress in spinning hollow fiber process.

The first reason has been mentioned previously. The higher TS corresponds to the less thickness of wall, whereas higher cooling rate results in shorter crystallizing time and more imperfect the crystalline. This leads to a lower crystallinity and melting temperature. In addition, the solidification of hollow fiber was faster under higher TS so that aggregations with stronger connection are formed. This was demonstrated in our previous article.[14] The isolated spherulites were connected if the cooling rate increased, and then the strength increased.

The second reason is elongational stress. Generally, higher TS produces a higher elongational stress that is favorable to the orientation and crystallization of PVDF. However, the absolute TS is very low (72 m min^{-1}) in this study comparing with TS (up to several thousand m min^{-1}) in chemical fiber industry.[22]Under such a low elongational stress, it is difficult for fiber to get a good orientation which showed a regular circle when investigated by WAXD. Hence, the influence of elongational stress on crystallization is minor comparing to the cooling rate. That is to say, the crystallization of PVDF is mainly influenced by the cooling rate. As the result of higher TS and cooling rate, the membrane presents a lower crystallinity and melting temperature. Good connection of aggregations without obvious orientation leads to a higher strength and elongation of breakage. Hence, the increase of TS in experimental range will be favorable to the enhancement of the strength.

However, the higher stress owing to higher TS is not easy to be relaxed completely and is frozen into the nascent hollow fiber in spinning process. Therefore, the hollow fiber under higher TS presents a higher shrinkage rate (Table I).

CONCLUSIONS

The effects of TS on the structure and properties of PVDF hollow fiber membrane were investigated. It was found that when TS was <41 m min^{-1}, it had no apparent effect on the structure of membrane. However, when TS increased to 72 m min^{-1}, the cross-sectional structure of membrane changed obviously and presented a uniform structure, whereas the change of surface structure was not obvious in the whole TS. Furthermore, both strength and elongation of breakage increased as TS increased, but the PWF and porosity changed slightly, and the hollow fiber became easy to shrink.

This work was supported by the Science and Technology Plans of Tianjin (10SYSYJC27900) and The National Natural Science Foundation of China (20874073).

REFERENCES

1. Lloyd, D. R.; Kinzer, K. E.; Tseng, H. S. *J. Membr. Sci.* **1990,** *52*, 239.
2. Doi, Y.; Matsumura, H. US Pat. 5,022,990, **1991.**
3. Takamura, M.; Yoshida, H. US Pat. 6,299,773, **2001.**
4. Hamanaka, K.; Shimizu, T. EP 1369168, **2003.**
5. Smith, S. D.; Shipman, G. H.; Floyd, R. M.; Freemyer, H. T.; Hamrock, S. J.; Yandrasits, M. A.; Walton, D. G. S. US Pat. 2,005,058,821, **2005.**
6. Gu, M. H.; Zhang, J.; Wang, X. L.; Tao, H. J.; Ge, L. T. *Desalination* **2006,** *192*, 160.
7. Gu, M. H.; Zhang, J.; Wang, X. L.; Ma, W. Z. *J. Appl. Polym. Sci.* **2006,** *102*, 3714.
8. Gu, M. H.; Zhang, J.; Xia, Y.; Wang, X. L. *J. Macromol. Sci. Phys.* **2008,** *47*, 180.
9. Su, Y.; Chen, C. X.; Li, Y. G.; Li, J. D. *J. Macromol. Sci. Pure.* **2007,** *44*, 305.

10. Su, Y.; Chen, C. X.; Li, Y. G.; Li, J. D. *J. Macromol. Sci. Pure.* **2007,** *44*, 99.
11. Ji, G. L.; Zhu, B. K.; Cui, Z. Y.; Zhang, C. F.; Xu, Y. Y. *Polymer* **2007,** *48*, 6415.
12. Ji, G. L.; Du, C. H.; Zhu, B. K.; Xu, Y. Y. *J. Appl. Polym. Sci.* **2007,** *105*, 1496.
13. Cui, Z. Y.; Du, C. H.; Xu, Y. Y.; Ji, G. L.; Zhu, B. K. *J. Appl. Polym. Sci.* **2008,** *108*, 272.
14. Li, X. F.; Lu, X. L. *J. Appl. Polym. Sci.* **2006,** *101*, 2944.
15. Li, X. F.; Wang, Y. G.; Lu, X. L.; Xiao, C. F. *J. Membr. Sci.* **2008,** *320*, 477.
16. Li, X. F.; Xu, G. Q.; Lu, X. L.; Xiao, C. F. *J. Appl. Polym. Sci.* **2008,** *107*, 3630.
17. Lu, X. L.; Li, X. F. *J. Appl. Polym. Sci.* **2009,** *114*, 1213.
18. Cha, B. J.; Yang, J. M. *J. Membr. Sci.* **2007,** *291*, 191.
19. Ji, G. L.; Zhu, L. P.; Zhu, B. K.; Zhang, C. F.; Xu, Y. Y. *J. Membr. Sci.* **2008,** *319*, 264.
20. Rajabzadeh, S.; Maruyama, T.; Sotani, T.; Matsuyama, H. *Sep. Purif. Technol.* **2008,** *63*, 415.
21. Rajabzadeh, S.; Teramoto, M.; Al-Marzouqi, M. H.; Kamio, E.; Ohmukai, Y.; Maruyama, T.; Matsuyama, H. *J. Membr. Sci.* **2010,** *346*, 86.
22. Chen, P.; Kotek, R. *Polym. Rev.* **2008,** *48*, 392.
23. Santoso, Y. E.; Chung, T. S.; Wang, K. Y.; Weber, M. *J. Membr. Sci.* **2006,** *282*, 383.
24. Shang, M.; Matsuyama, H.; Teramoto, M.; Lloyd, D. R.; Kubota, N. *Polymer* **2003,** *44*, 7441.
25. Marega, C.; Marigo, A. *Eur. Polym. J.* **2003,** *39*, 1713.
26. Cabasso, I.; Klein, E.; Smith, J. K. *J. Appl. Polym. Sci.* **1976,** *20*, 2377.
27. Aptel, P.; Abidine, N.; Ivaldi, F. *J. Membr. Sci.* **1985,** *22*, 199.
28. Wang, K. Y.; Li, D. F.; Chung, T. S.; Chen, S. B. *Chem. Eng. Sci.* **2004,** *59*, 4657.
29. Cao, C.; Chung, T. S.; Chen, S. B.; Dong, Z. *J. Chem. Eng. Sci.* **2004,** *59*, 1053.